Magnetic Field Measurements on the Self Magnetic Pinch Diode At SNL using Zeeman Splitting

S.G. Patel, M.D. Johnston, T.J. Webb, M. Mazarakis, N. Bennett, D.J. Muron, M.L. Kiefer

Sandia National Laboratories, Albuquerque, NM 87185

Y. Maron

Weizmann Institute of Science, Rehovot, Israel 76100

R.M. Gilgenbach

University of Michigan, Ann Arbor, MI 48109 USA

NRL Seminar, Dec. 2015

SAND2018-9524PE

Exceptional service in the national interest

Sandia National Laboratories

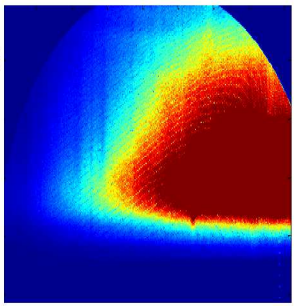

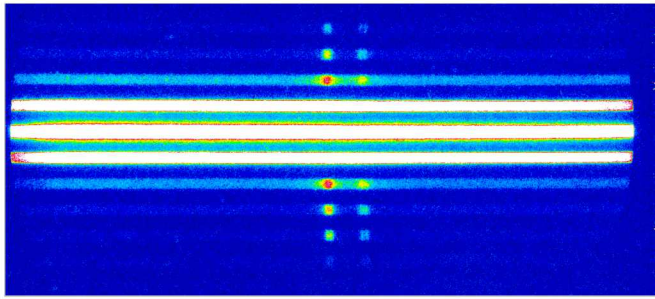

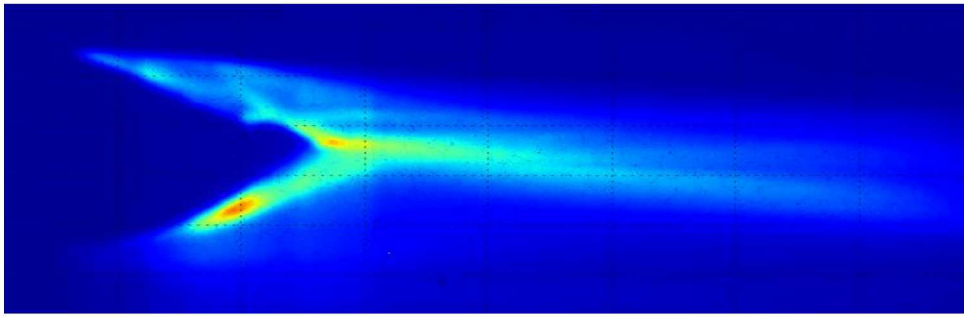

U.S. DEPARTMENT OF ENERGY

NNSA National Nuclear Security Administration

Sandia National Laboratories is a multi-program laboratory managed and operated by Sandia Corporation, a wholly owned subsidiary of Lockheed Martin Corporation, for the U.S. Department of Energy's National Nuclear Security Administration under contract DE-AC04-94AL85000.
SAND No. 2011–XXXXP.

Outline

Sandia National Laboratories

- Motivation
- RITS Accelerator and the SMP Diode
- Zeeman Effect Background
- Experimental Setup
- Spectrum Deconvolution
- Temperature and Density Measurements
- Measured Current and Magnetic Field Profile
- Conclusions and Future Work

Motivation

Sandia National Laboratories

- Determine the current distribution in the Self Magnetic Pinch (SMP) Diode using Zeeman splitting to measure local magnetic fields.
- Benchmark LSP simulations
- Improve diode designs
- Provide a proof of principle B-field measurement for future Z convolute measurements

1. LSP Suite: Particle-in-Cell (PIC) code, http://www.mrcwdc.com/LSP/index.html

RITS-6 Accelerator

- RITS uses a 6 stage induction voltage adder to deliver power to the load
- Diode Parameters
  - ~8.0 MV
  - 130-160 kA
  - Few mm spot size
  - 40-50ns Radiation Pulse with Foil
  - 30-40ns Radiation pulse with bare converter

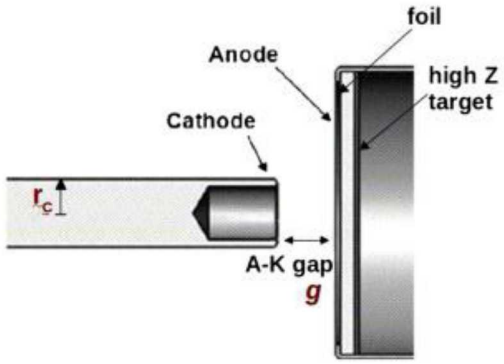

Diode Configuration[1]

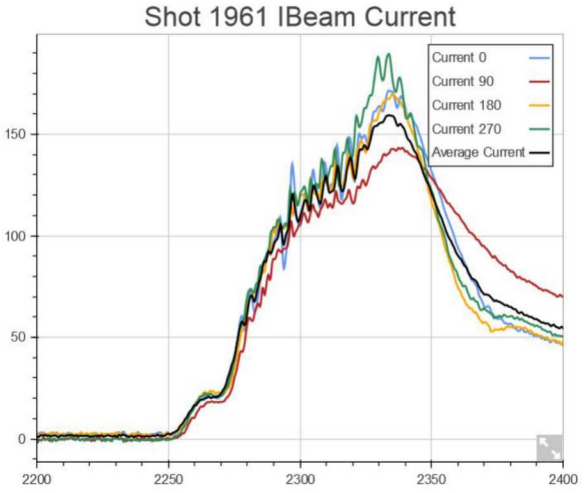

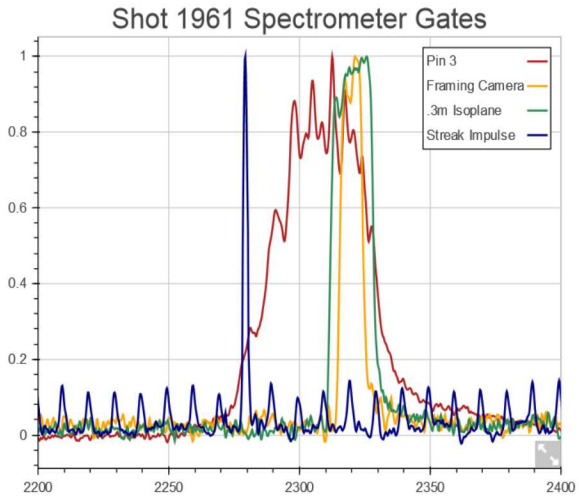

1. N. Bruner et al. 2011
2. N. Bennet et al. 2014

SMP Diode

- The SMP diode produces an electron beam for x-ray radiography.
- The beam pinches from its self B-field as it crosses the A-K gap
- Plasmas form on the electrode surfaces and expand into the AK gap, decreasing the diode impedance over time[2]

SMP diode simulation[3]

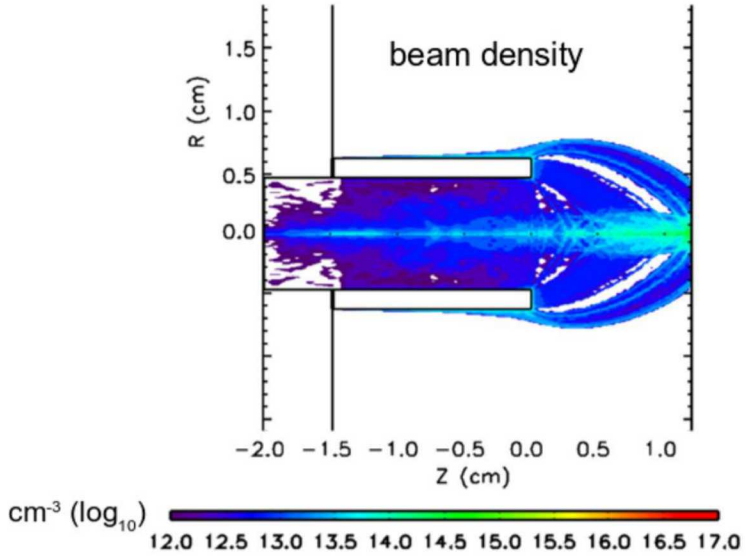

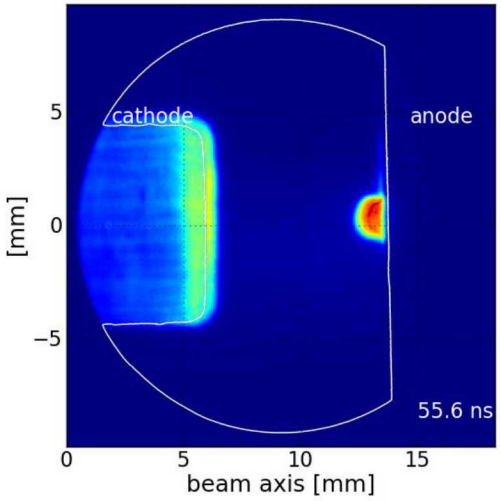

3. N. Bennet et al. 2015

B-field Diagnostics

Sandia National Laboratories

- B-dots are used behind the cathode to measure the diode current.
  - However, B-dots are limited to measuring outside the AK gap
- Faraday rotation measurements require an external polarized light source and the data is line integrated along the laser path.
- Zeeman splitting measurements can be localized using dopants and can be measured within the plasma.
  - Requires high enough densities to measure strong signals, but low enough densities and temperatures to not be overshadowed by Stark or Doppler broadening

Zeeman Splitting

Energy Diagram

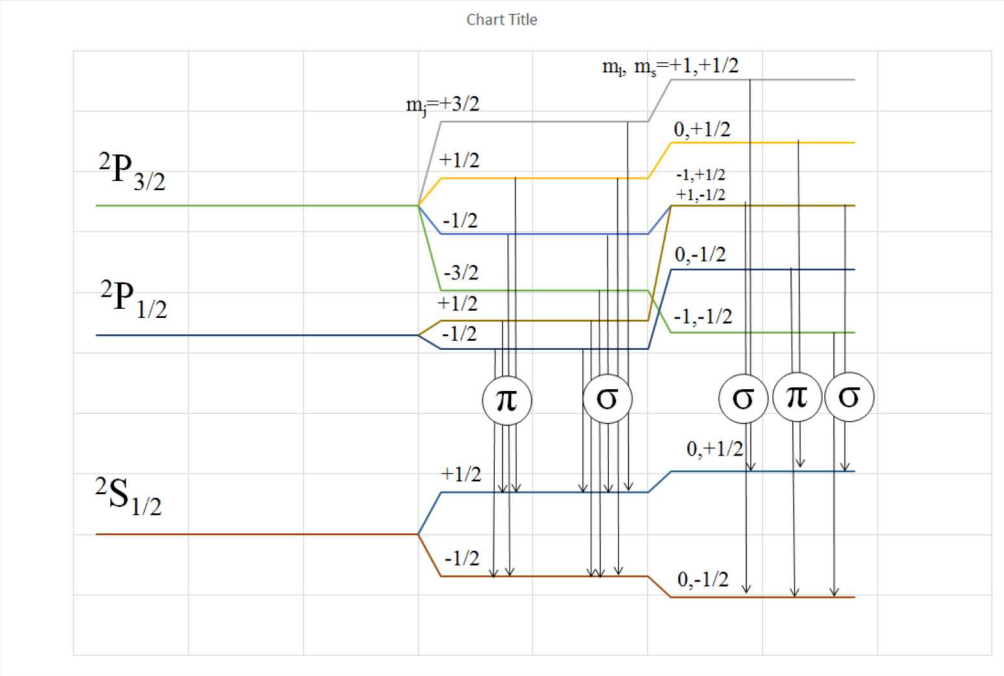

- Zeeman splitting can be used to infer local B-fields at the plasma location.
- Weak field:
  - $\Delta E = g m_j \mu_B B$
- Strong Field:
  - $\Delta E = (m_l + 2m_s)\mu_B B$
- For small B-fields it is advantageous to look parallel to the field lines, as pi components are not visible.

Zeeman Effect Simulated Spectra

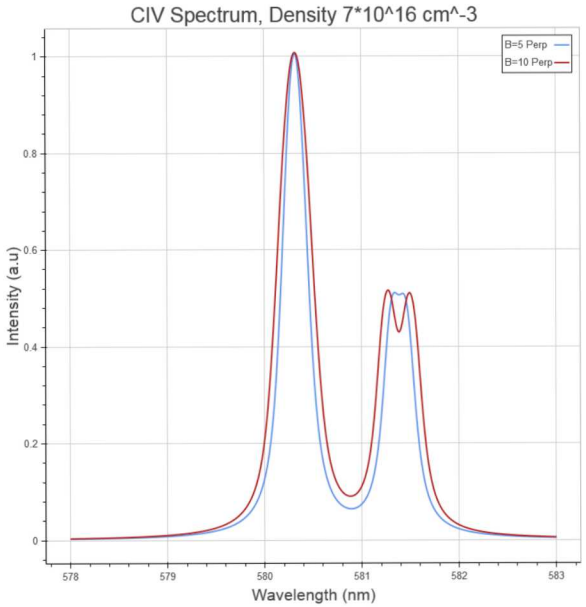

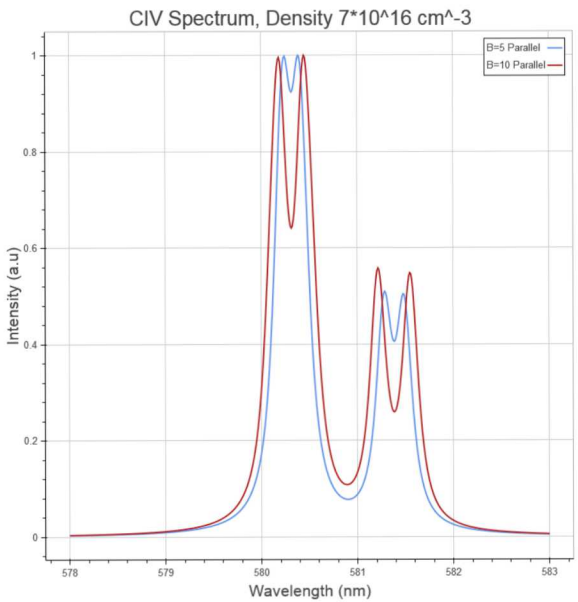

- Perpendicular and parallel lines of sight plotted using a resolution of 0.06 nm for the CIV doublet.
- The ^2S-^2P doublet is particularly useful for this effect because the $P_{1/2}$-$S_{1/2}$ transition is always slightly more broadened than the $P_{3/2}$->$S_{1/2}$ transition[4,5].

4. E. Stambulchik et al. 2007
5. S. Tessarin et al. 2011

Potential Emission Lines

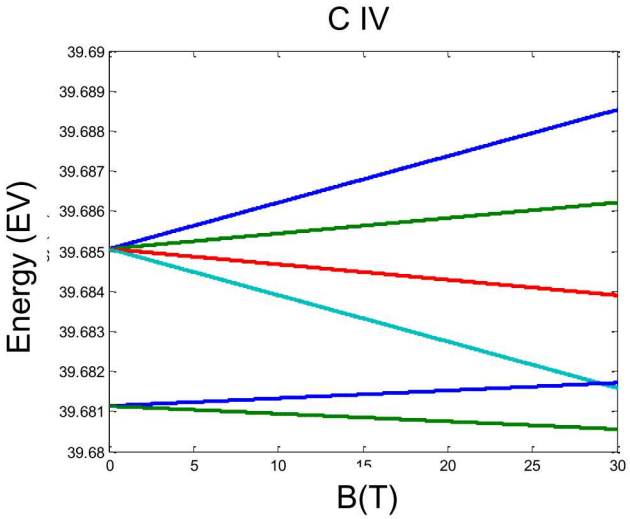

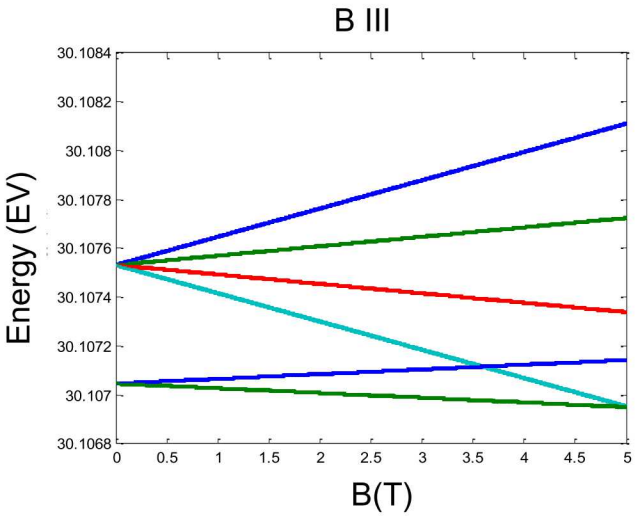

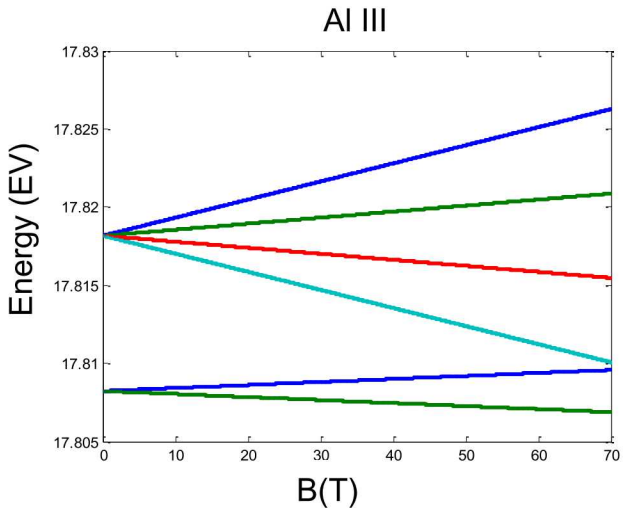

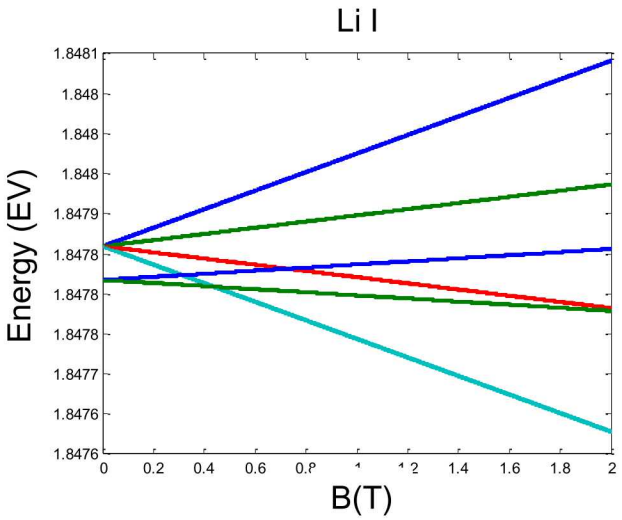

- Lines that transition to the Paschen-Back regime at low fields may be useful.
- C is a contaminant possibly from the oil used on the knob to prevent emission
- Potential dopants include B III, Si IV, Li I, Na I
- Dopants would help isolate the fiber position.

Line Broadening

- Natural Line width
  - Due to the energy time uncertainty principle. Very small and most often overshadowed by other broadening mechanisms.
- Thermal Doppler Broadening
  - $\Delta\lambda = \lambda_o 2\sqrt{\frac{2(ln2)kT}{m_o c^2}}$, small compared to the instrument broadening.
- Instrument broadening: ~0.065nm
  - Determined from an Hg calibration lamp.
- Stark Broadening
  - A type of pressure broadening due to coulomb interactions.
- Magnetic Field
  - Zeeman effect when the B field is not strong enough or the densities too high to fully split the line.

Experimental Setup

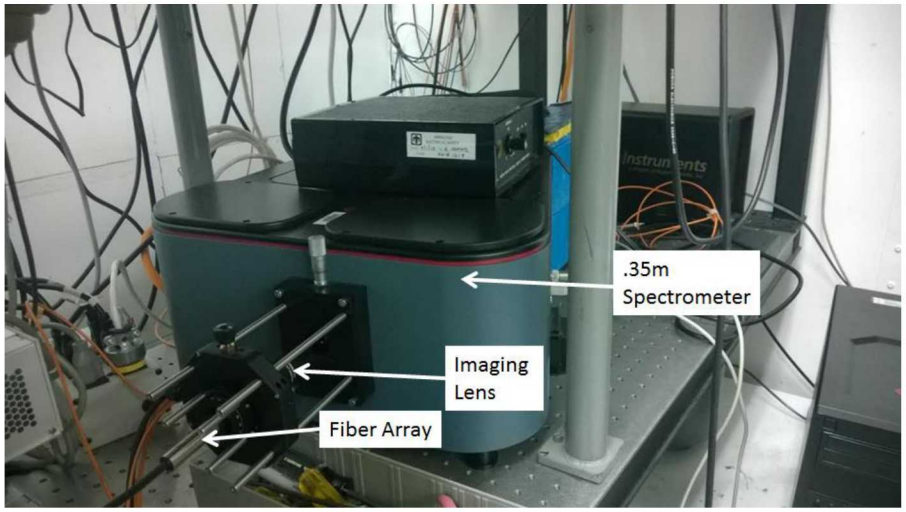

- A 0.35m lens coupled spectrometer is used with a 2400 g/mm grating. (~0.6 A resolution)
- Gated ICCD Camera: 10-15 ns gate.

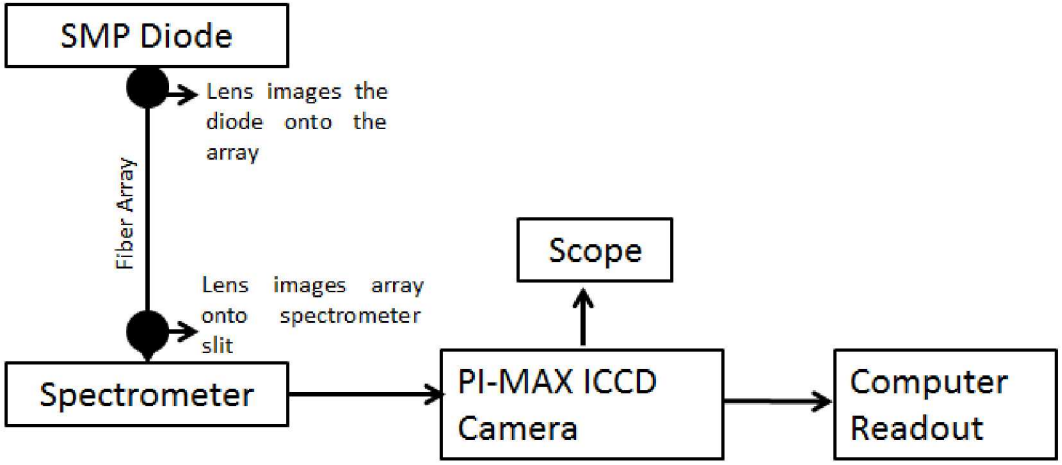

Experimental Setup

- Fibers are focused to a 1mm spot across the surface of the foil or converter where the B-fields are the largest.
- Spectra are collected toward the end of the radiation pulse, just before impedance collapse to maximize light.

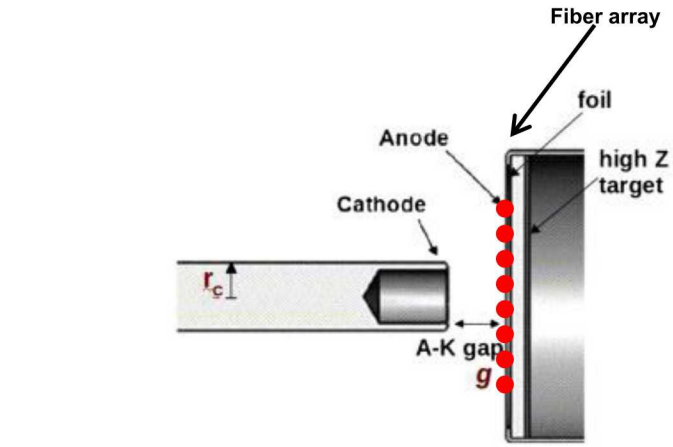

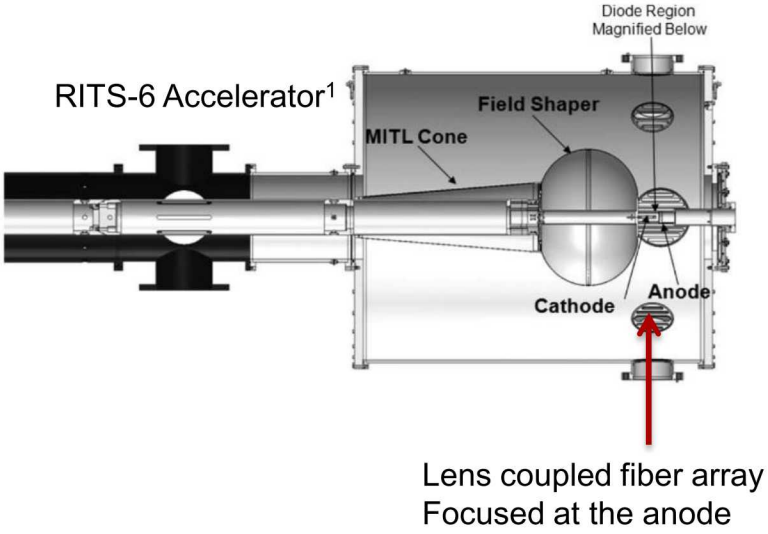

Streaked Spectra

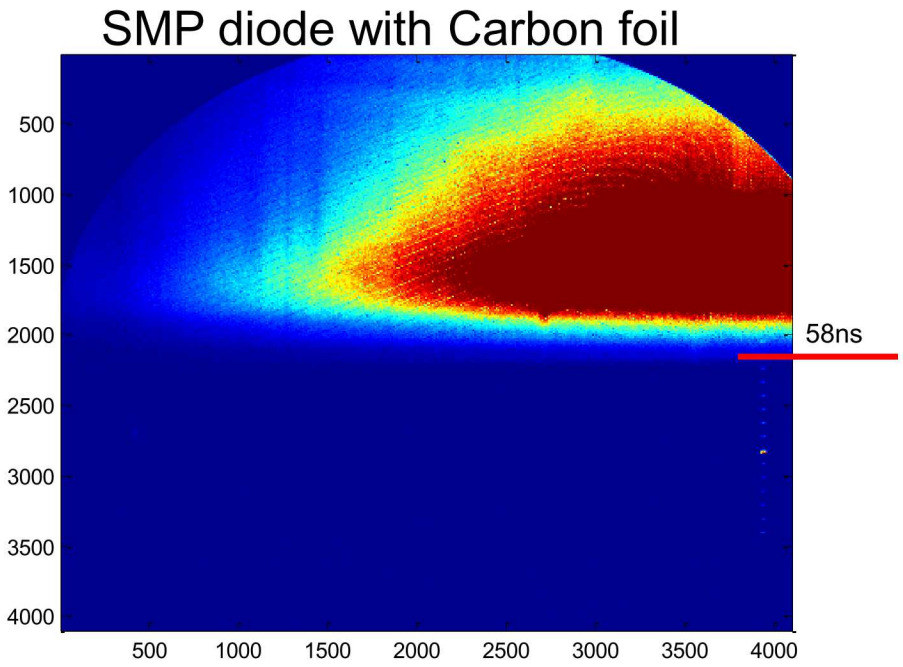

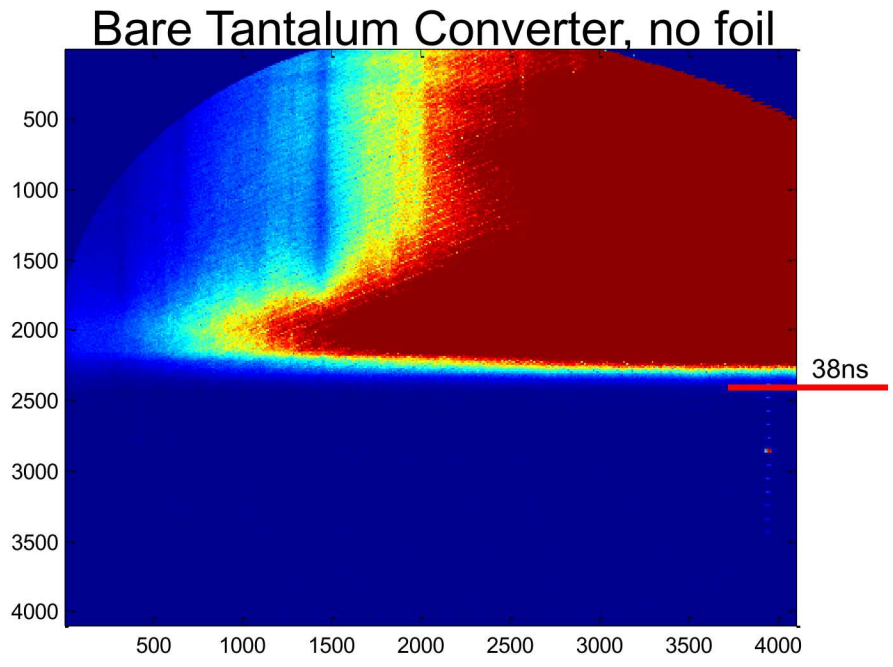

- 150 g/mm,1m spectrometer
- 1-2mm off axis, skimming the surface of the anode
- The foil prevents plasma from expanding into the gap and shorting the AK gap
- The foil takes time to ionize, as a result the spectrometer collects less light during the radiation pulse when compared to a bare convertor.
- A bare or coated converter plate was used in most of the Zeeman splitting measurements, which resulted in slightly shorter pulse widths (30-40ns instead of 40-50ns)

Spectrum Evolution

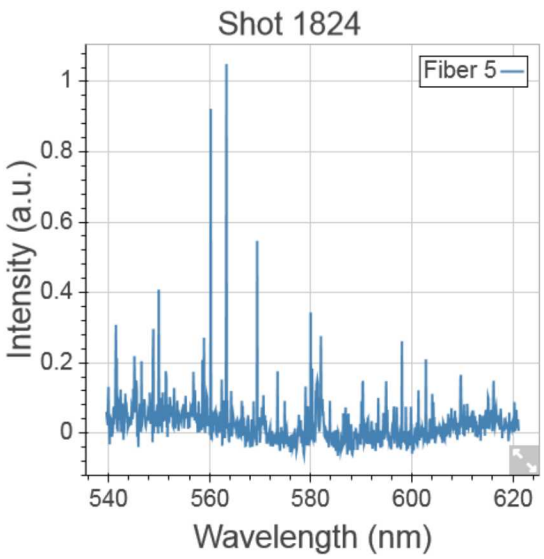

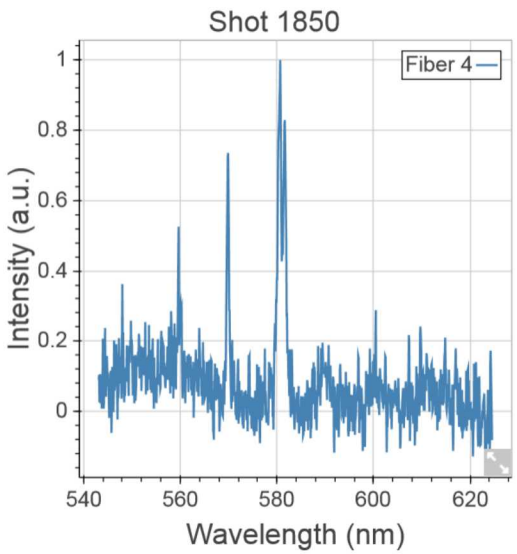

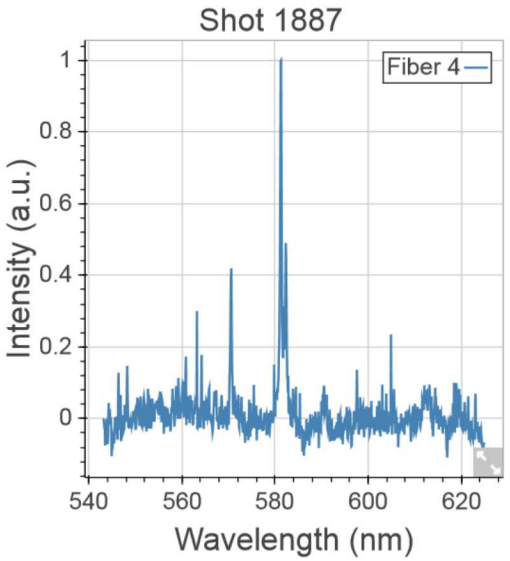

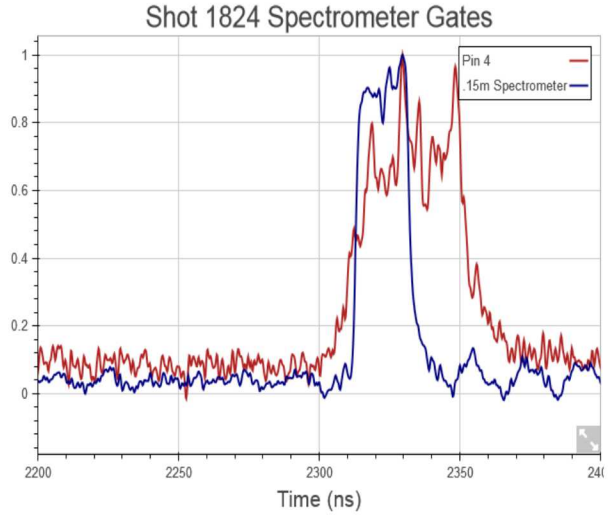

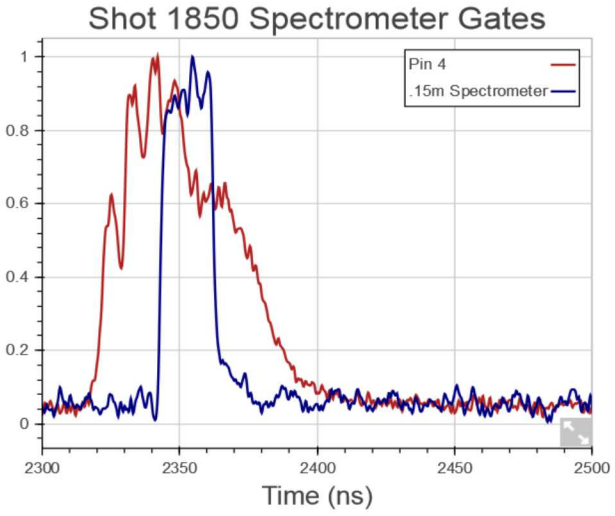

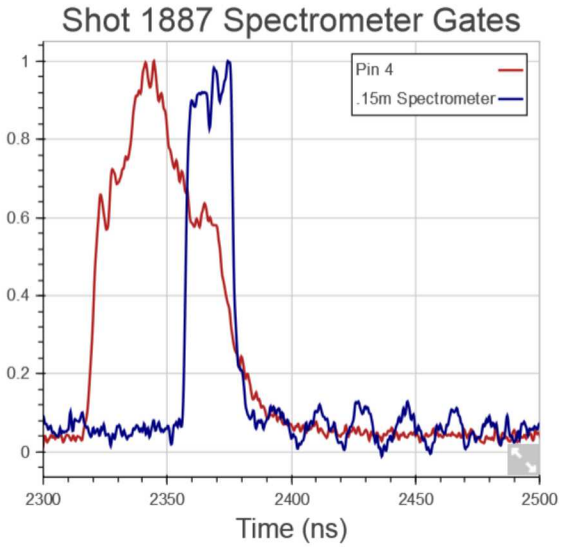

Resolution

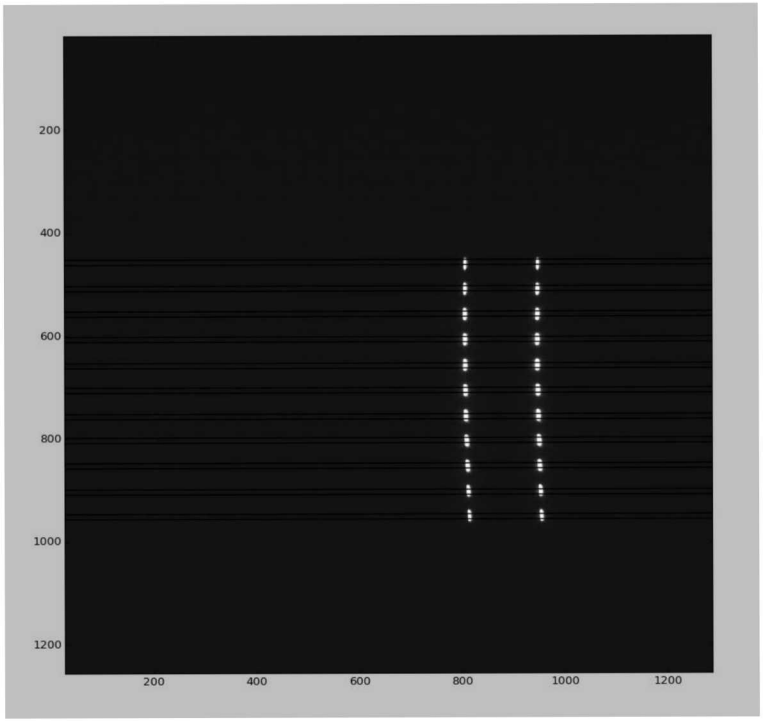

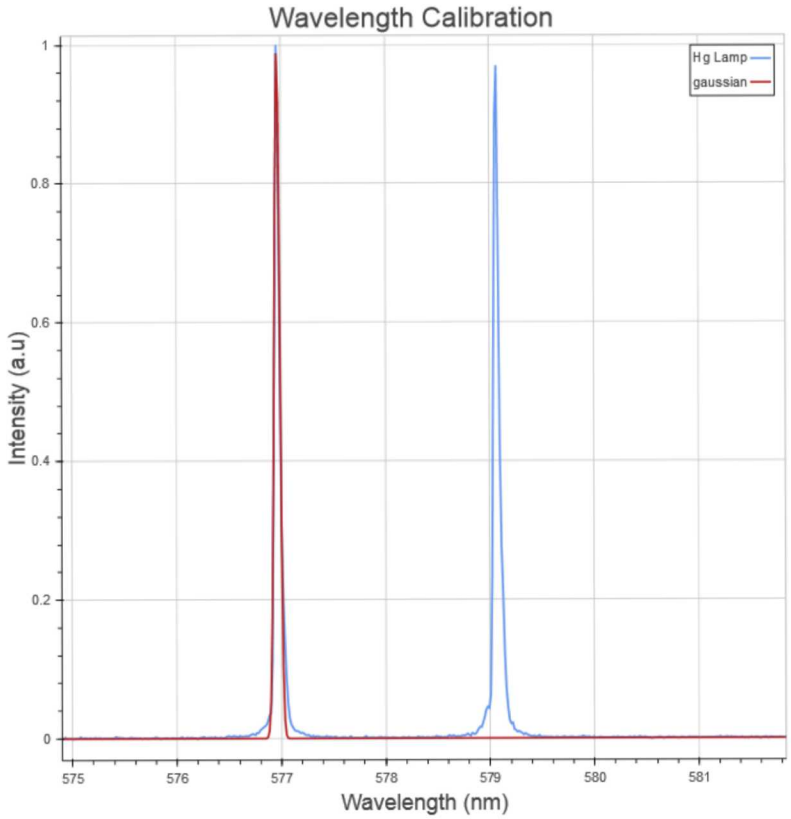

- Use an Hg lamp to calibrate wavelength and determine the instrument resolution for each shot. Instrument resolution is about 0.065nm.

Camera Response Calibration

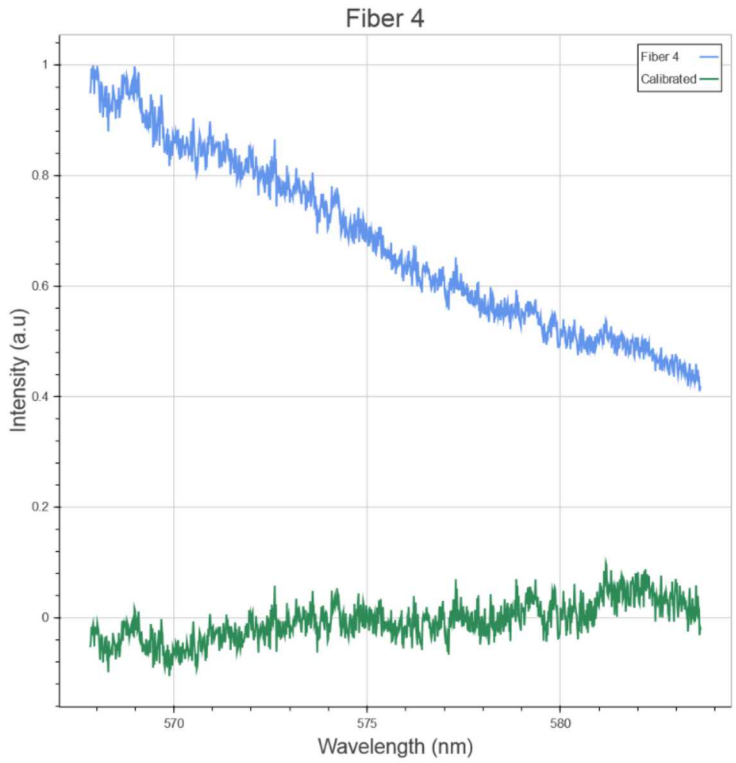

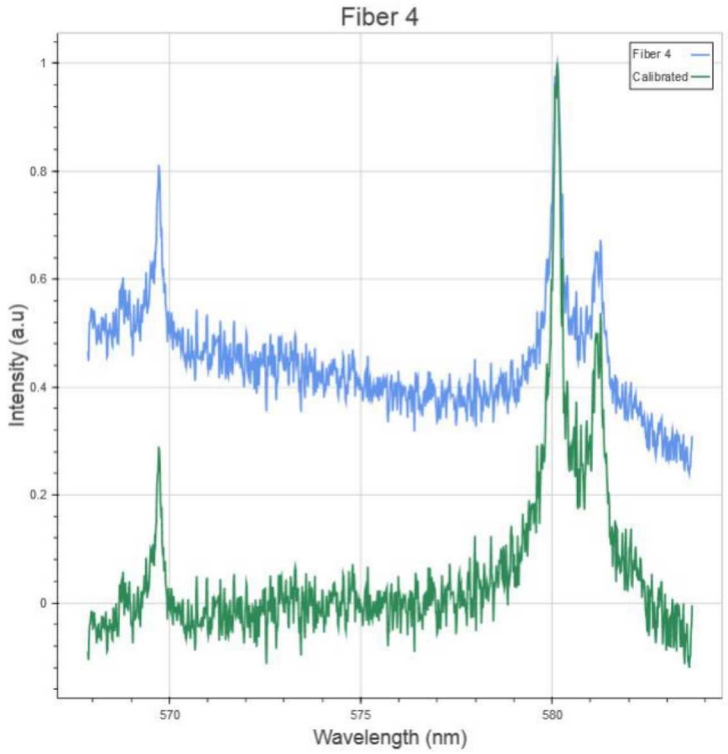

- Spectra taken with an integrating sphere of known radiance.
  - Scatters light within a hollow sphere. Multiple reflections within the sphere results in a uniform light source.
  - Tungsten light source

Distance from Axis

- It is difficult to align the fibers so that the center fiber of the array is on the axis of the beam.
- A Gaussian profile is fit to a vertical lineout of the spectra.
- The peak is considered to be the axis for this analysis.

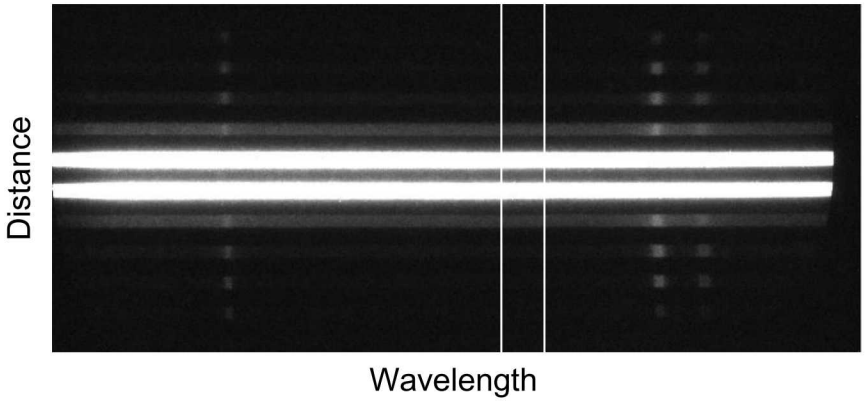

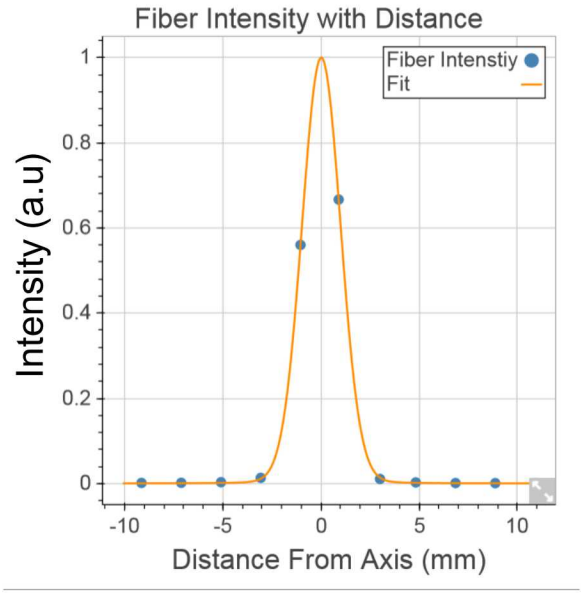

Zeeman Splitting Fits

- Each component of the Zeeman lines are broadened by density and the instrument, resulting in a voigt profile
- Zeeman splitting is fit assuming:
  - Gaussian spot intensity
  - Fiber is well focused for a 1cm chord
    - Sigma and pi line components are factored into the fit
  - Cylindrical symmetry of e-beam
  - Optically thin plasma, p3/2->s1/2 and p1/2->s1/2 ratio is 2

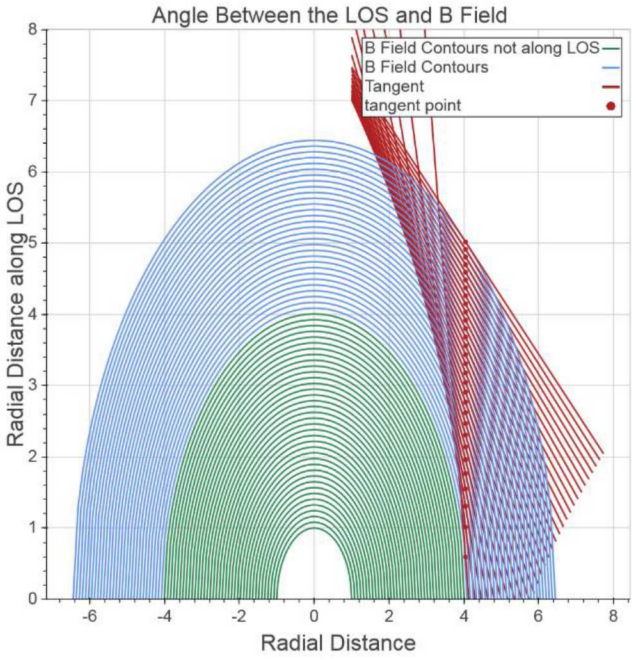

Parallel and perpendicular components change the line profiles. Line of sights closer to the center contain more pi components than lines further from the axis.

Ultra 8 Framing Camera

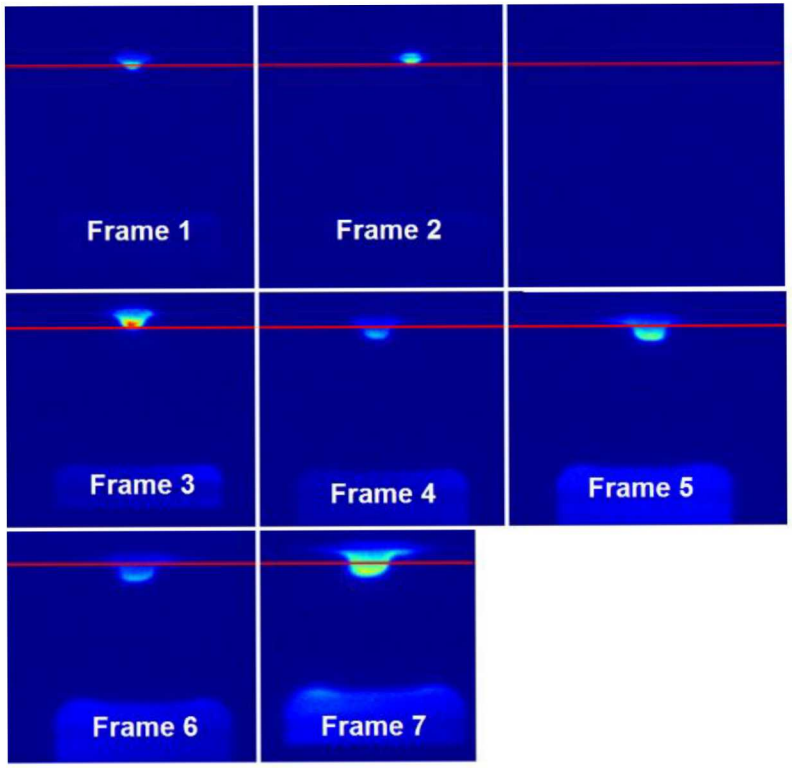

- Each frame is 10 ns apart.
- Frame 1 begins just after the start of the radiation pulse

Doppler Shift

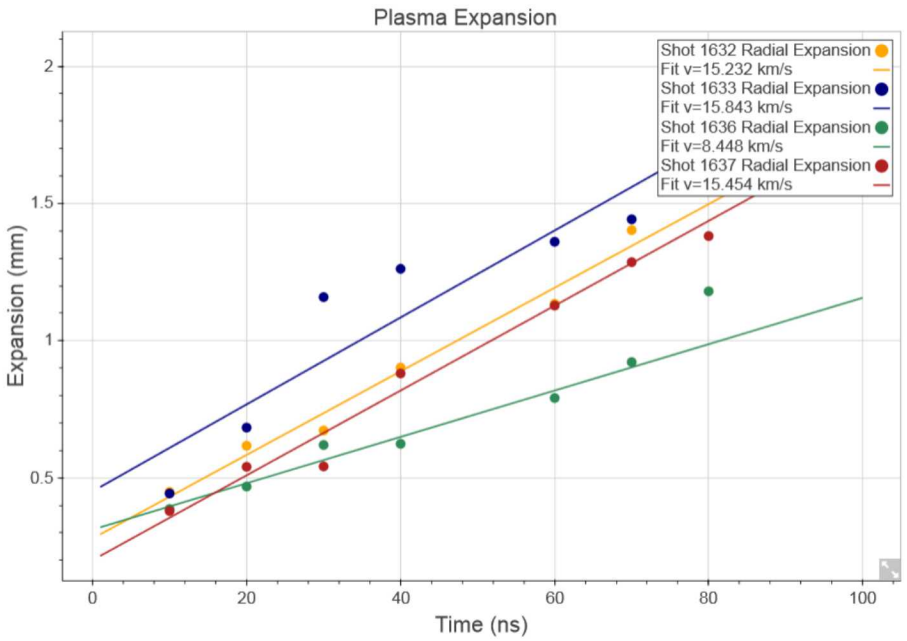

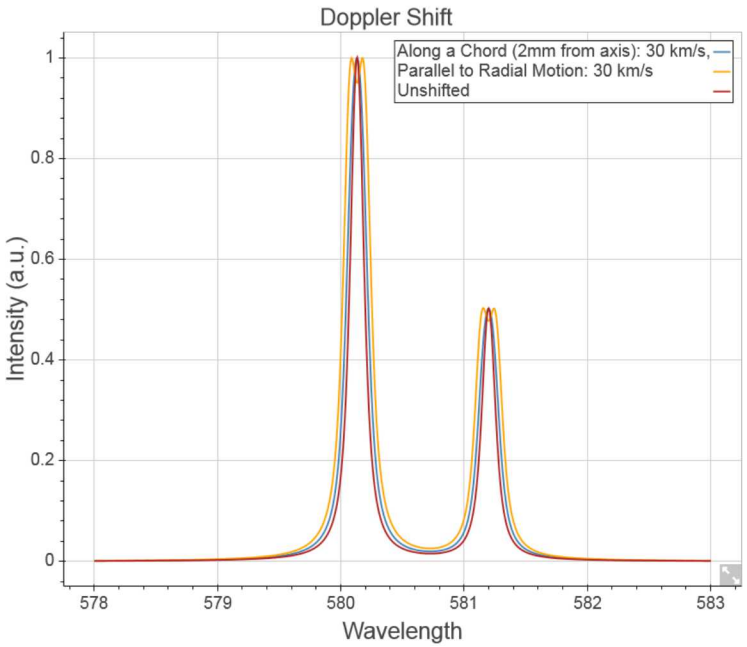

- Radial velocities are likely too small to affect the measured Zeeman splitting.
- The outer fibers at ~10mm would require 60-80 km/s to measurably differ from the Stark broadening

Comparison between fits

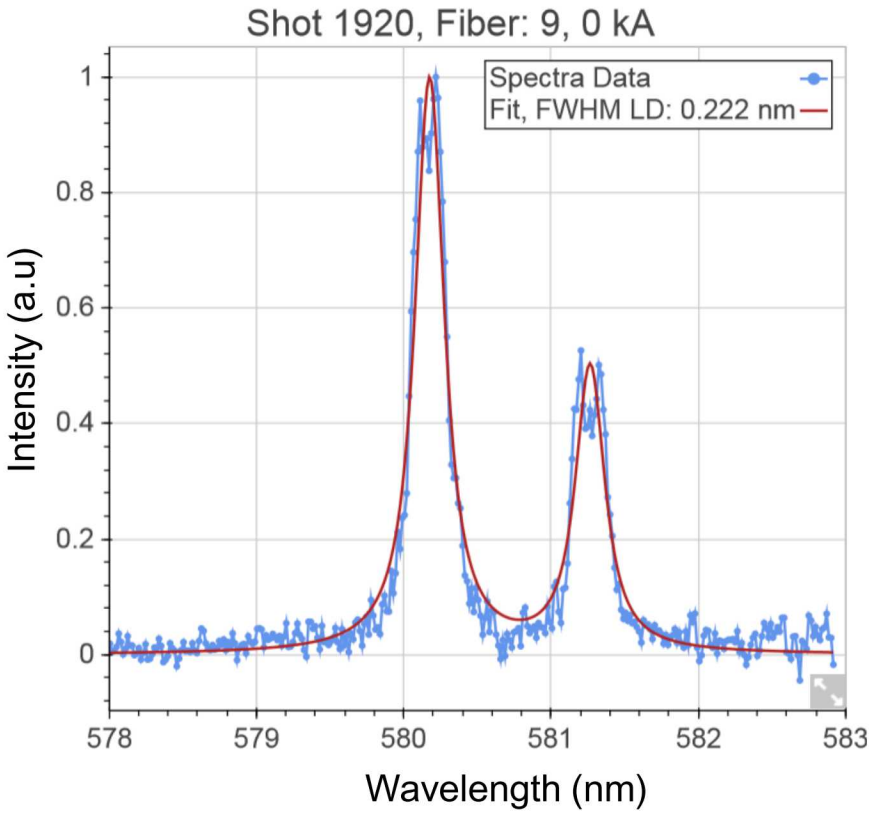

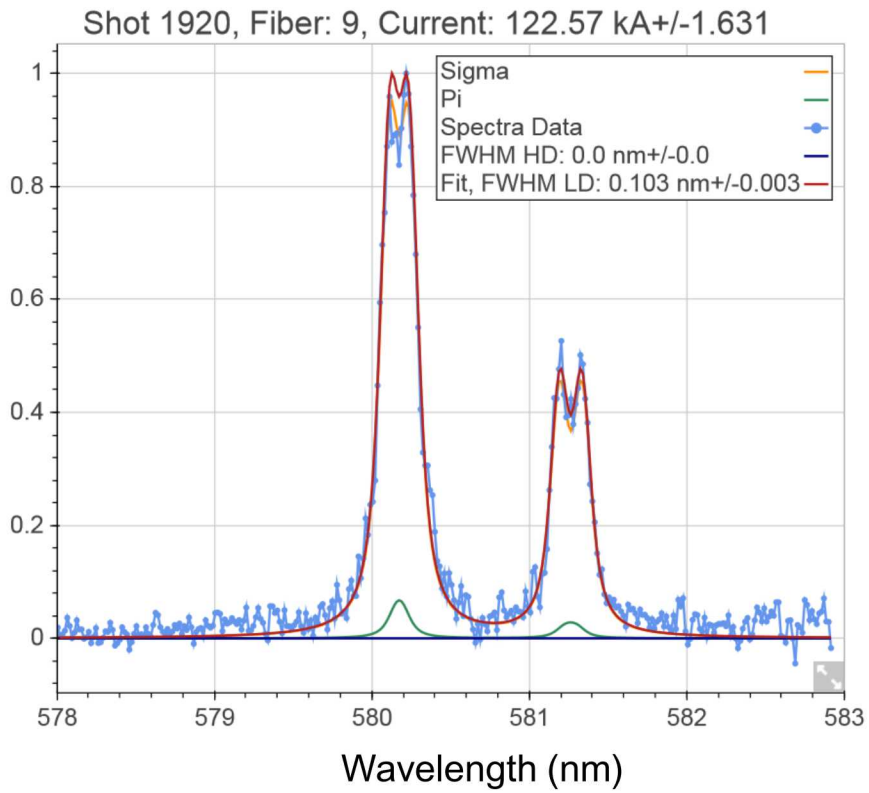

- Outer fiber fit with and without a magnetic field.

Comparison between fits

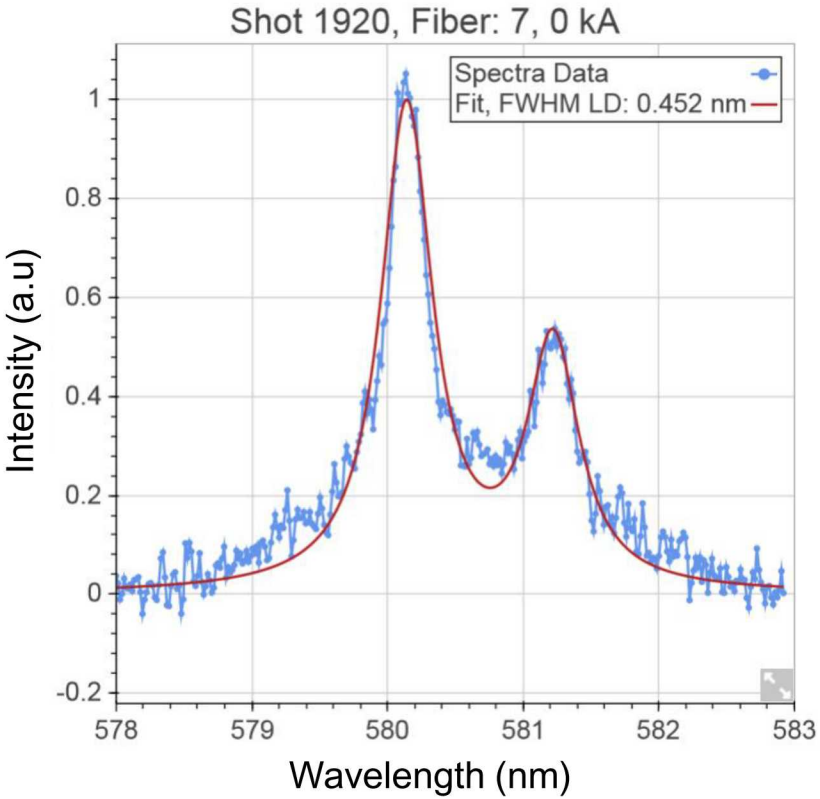

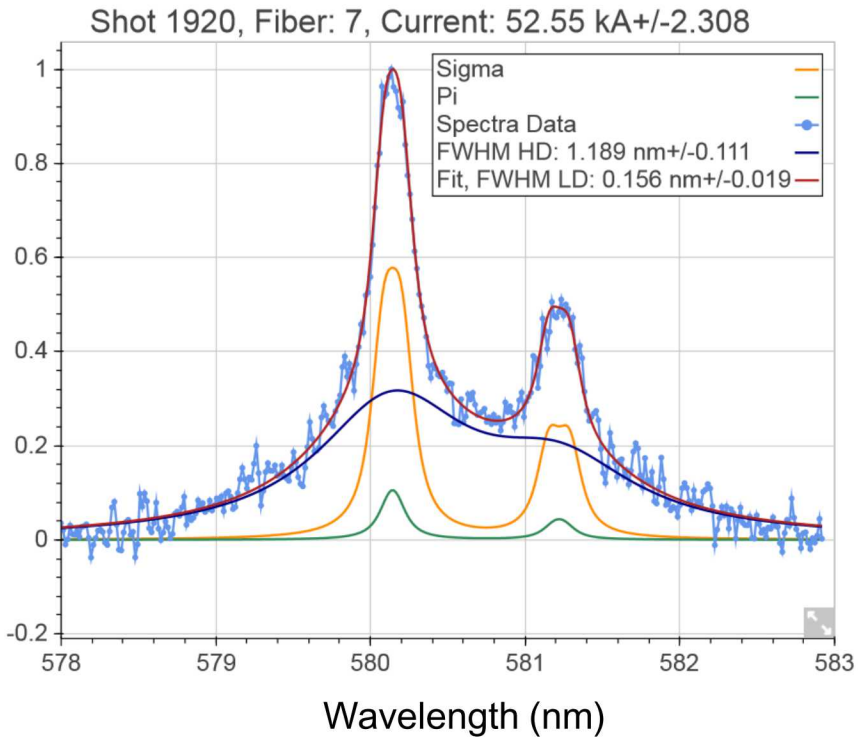

- A fit of a spectrum taken close to the axis with and without the magnetic field.
- Doublet broadening and the wings are more accurately fit.

Temperature and Density

Sandia National Laboratories

- Temperatures are determined by using consecutive ionization state line ratios.
- Densities are determined by fitting line widths to PrismSpect.
  - Uses a semi-empirical approximation[8]
  - The width is a weak function of temperature.

Temperature and Density

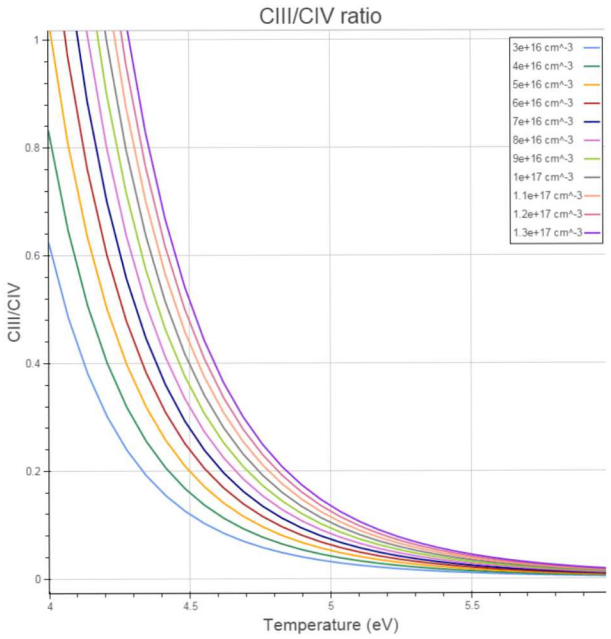

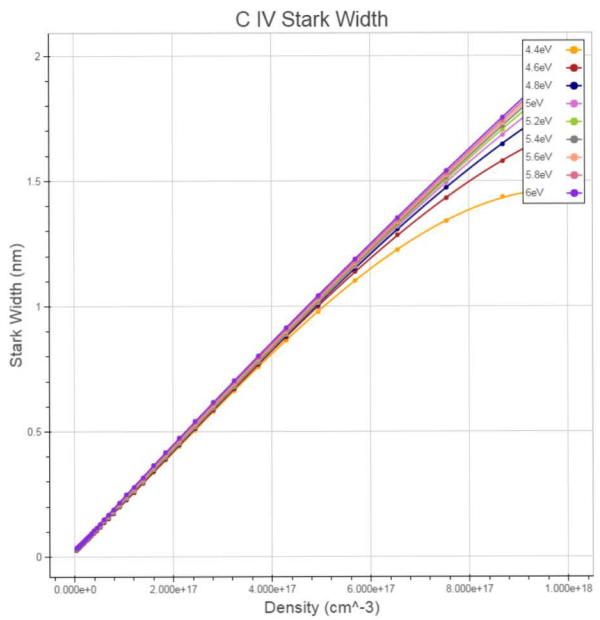

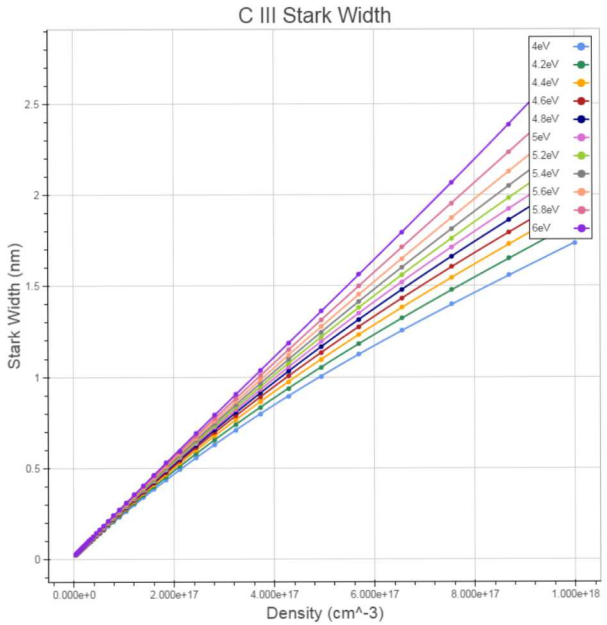

- Densities are from PrismSpect, a collisional radiative code.
- Temperatures vary by about .5-1 eV in the range both CIII and CIV lines are visible.
- CIV stark width does not vary much with temperature until widths>1nm
- In spectra without a temperature estimate CIV densities may still be reasonably estimated at densities below $6*10^{17}cm^{-3}$

Temperature and Density

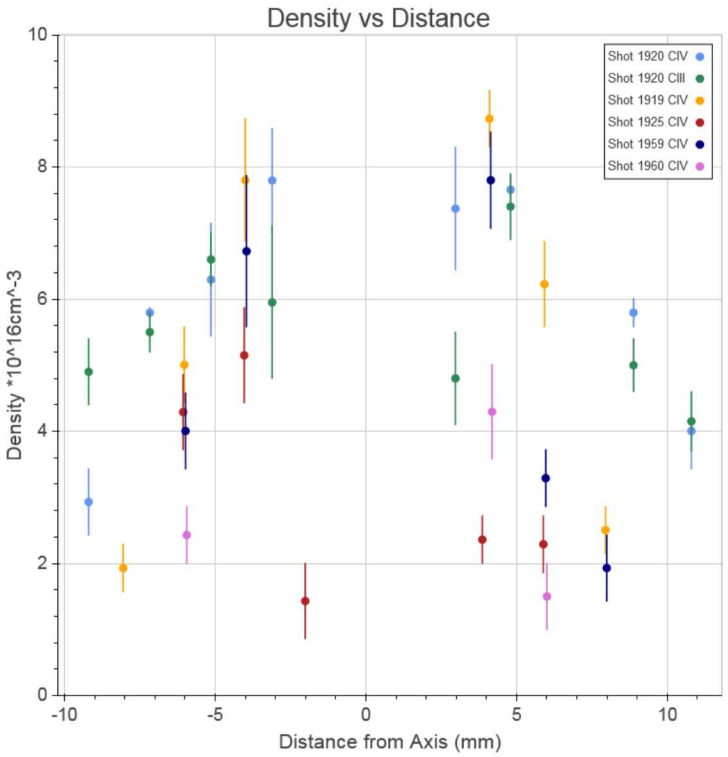

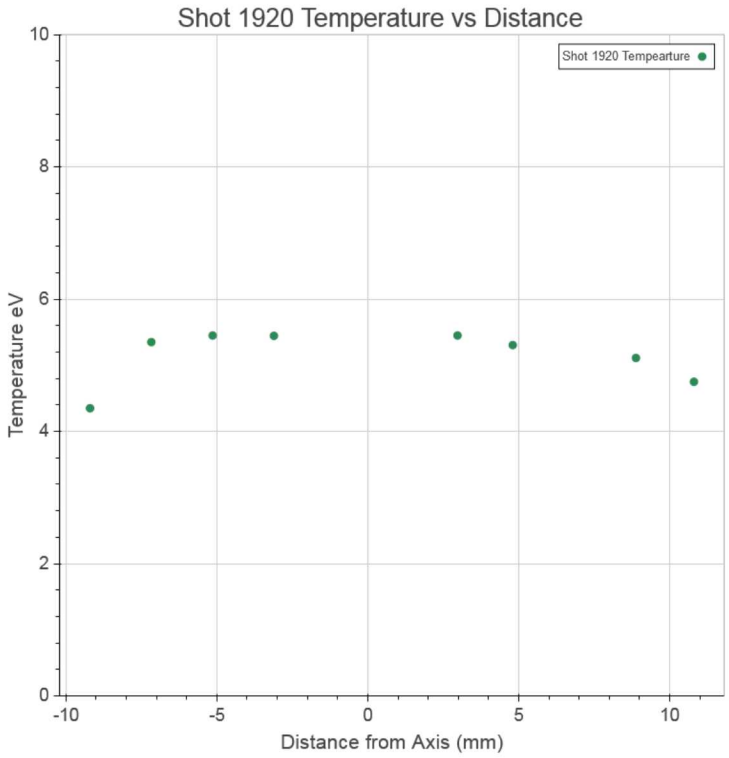

- A Voigt profile is used to approximate the line shape. The Gaussian part is from the instrument broadening, and the Lorentzian FWHM is fit and the density is calculated from Prismspect.
- Low density components shown after fitting Zeeman splitting. Errors shown are approximated from the fit uncertainty.
- Temperature is from CIII/CIV and is roughly 5.5eV across the anode. Densities are ~mid $10^{16}cm^{-3}$ and drop with distance from the axis.

Density Gradients

- High density component differs by about an order of magnitude from the low density component.
- Low density CIV component is much closer to the CIII densities and is therefore more likely to be in similar locations.
- The low density component is used for the temperature estimate.

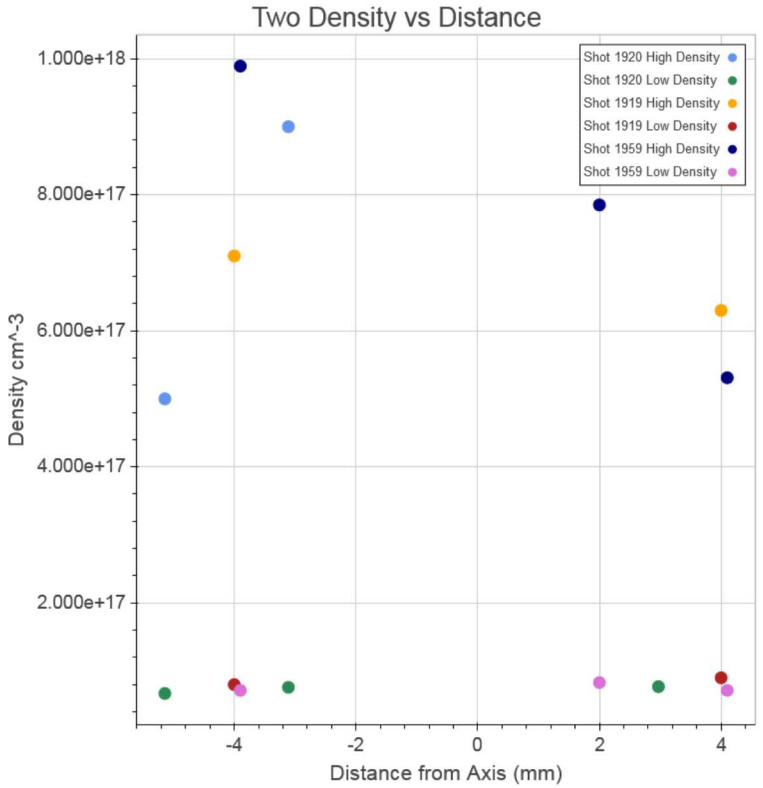

Electron Density from H-alpha

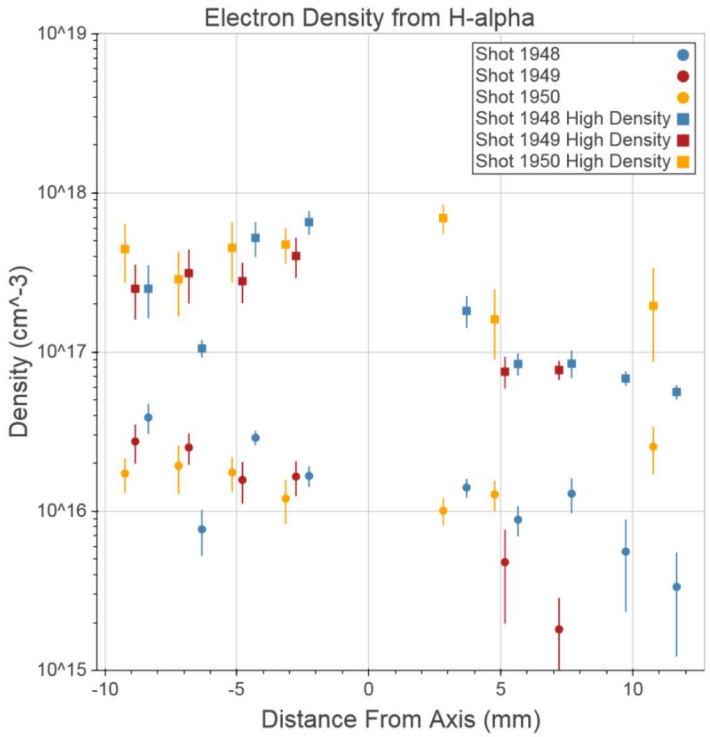

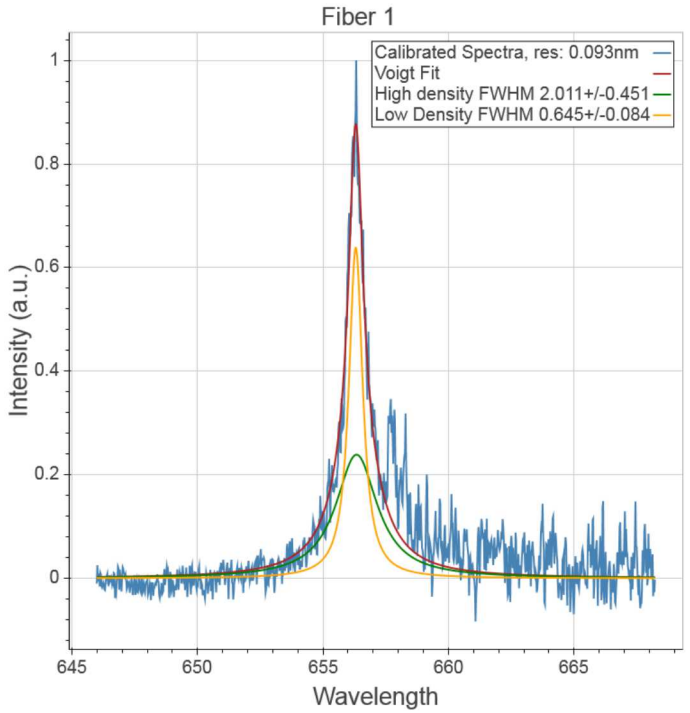

- Densities from Griem's ST model
- Suggests more H-alpha is present closer to the surface than CIV since the broad high density component is present across the entire fiber array.

Density Gradients

- Switched to a 100 um fiber array, focused to a .5 mm spot.
- More line broadening as this array images closer to the surface
- Shot 2027: Al Coated Ta

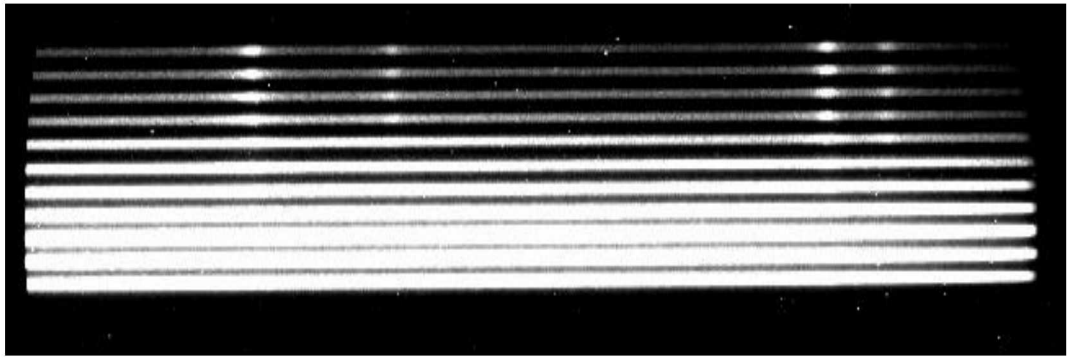

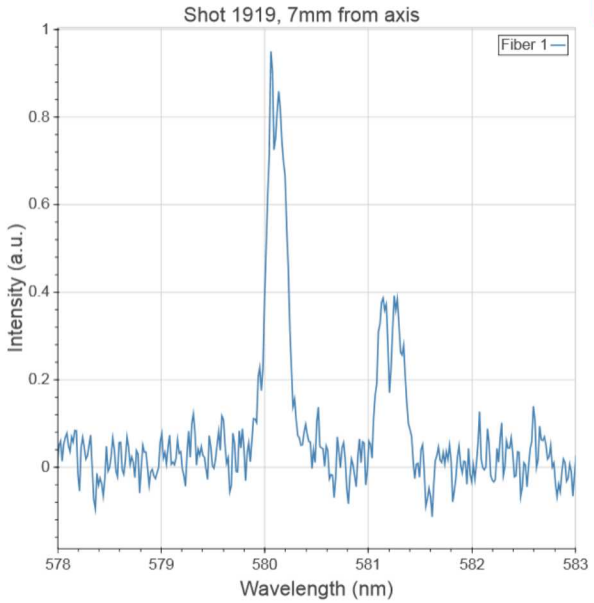

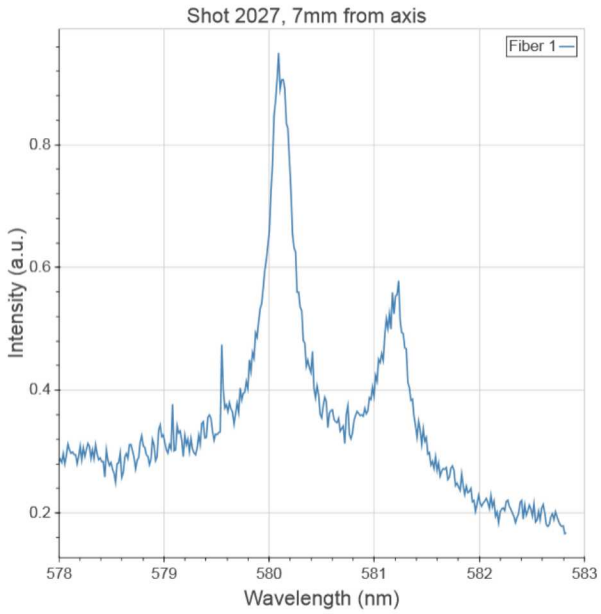

Density Gradients

Shot 2028, Al Coated Ta

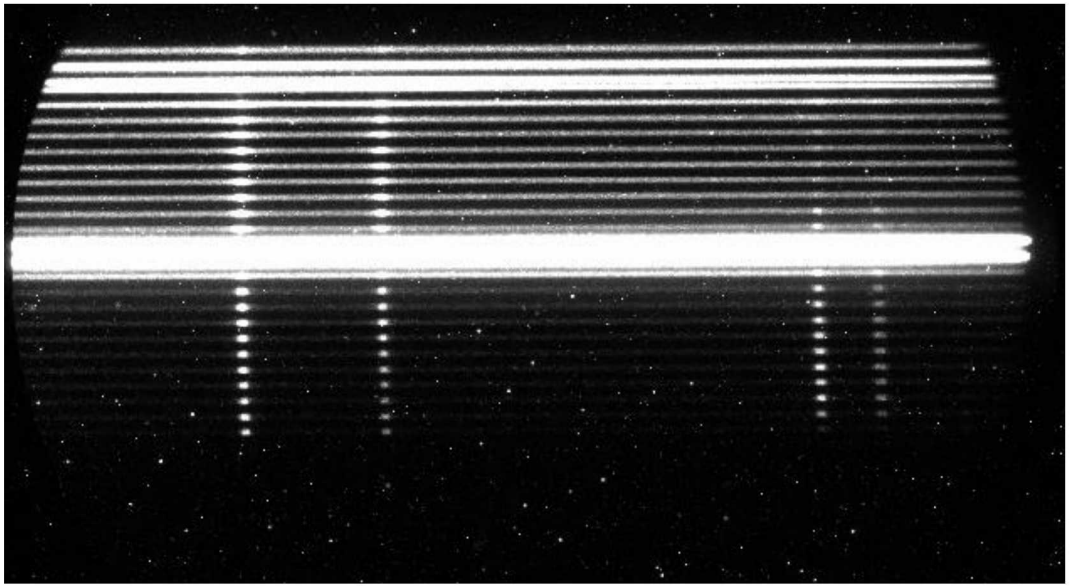

On the anode surface

~.5mm off the surface

Fiber array consists of 26 fibers, focused to a .5 mm spot parallel to the anode surface.

The array is designed to separate the high density surface plasma from the lower density plasma that is used to fit Zeeman splitting.

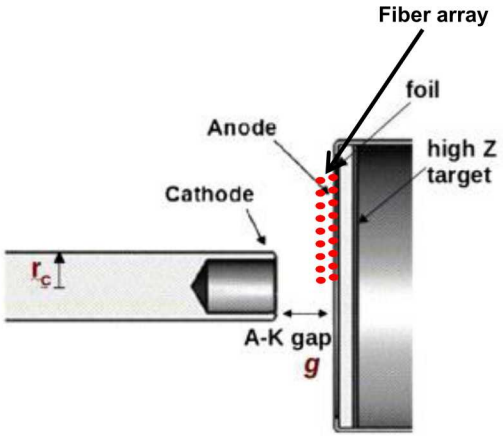

Shot 1919

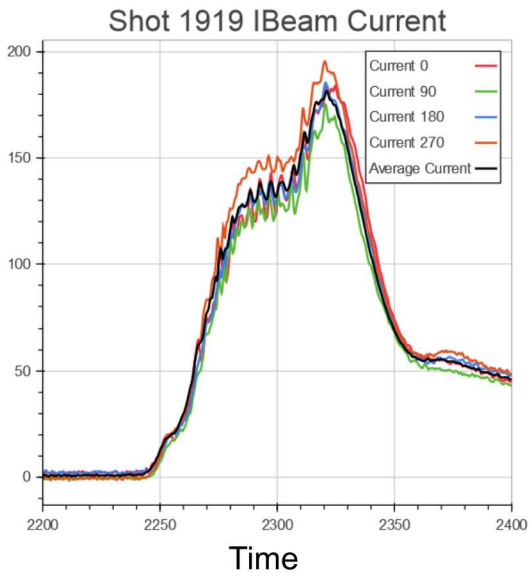

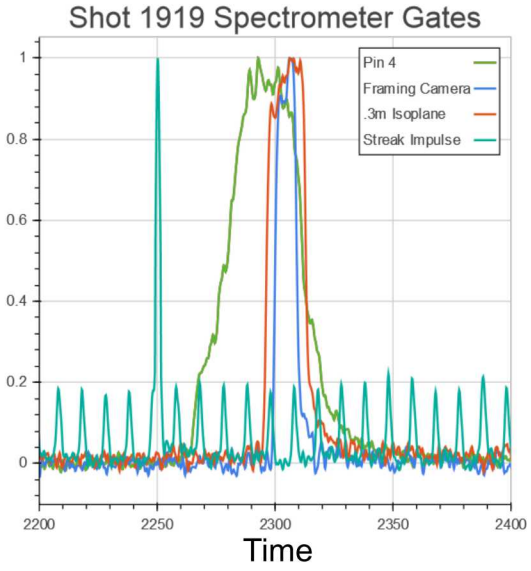

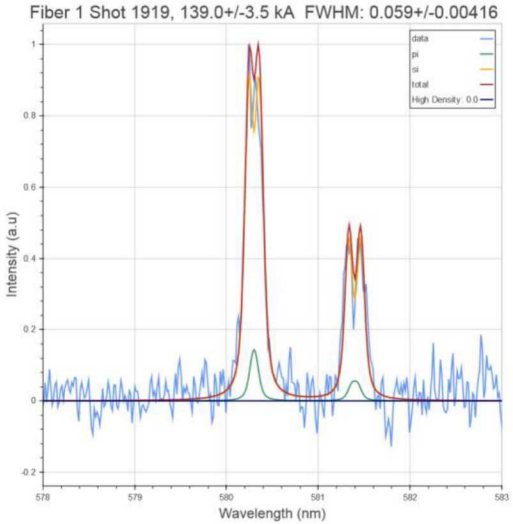

- Carbon coated Tantalum converter plate
- CIV lines visible

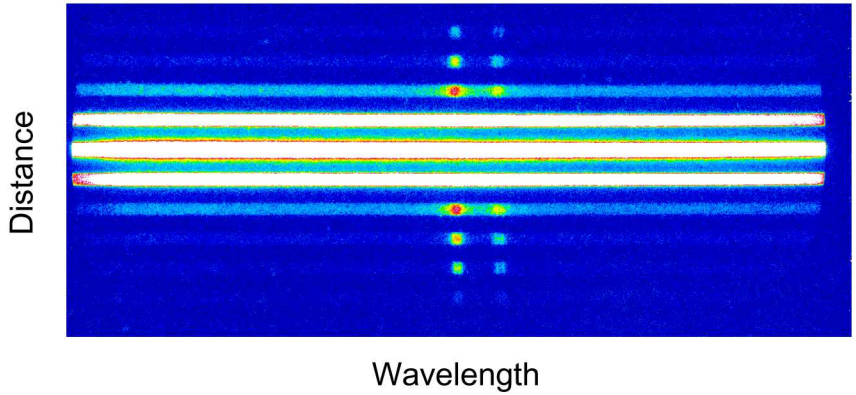

Shot 1925

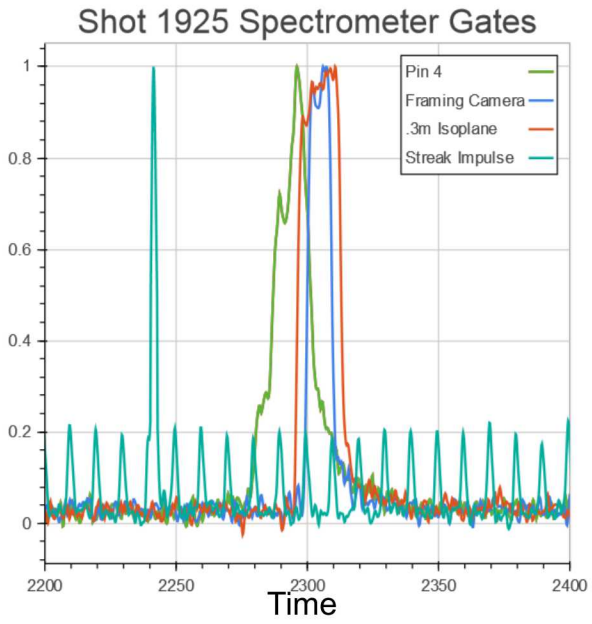

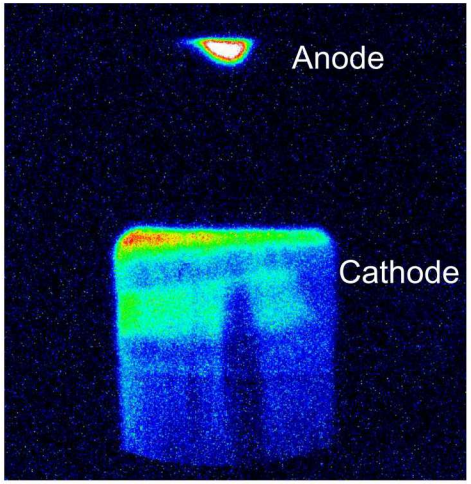

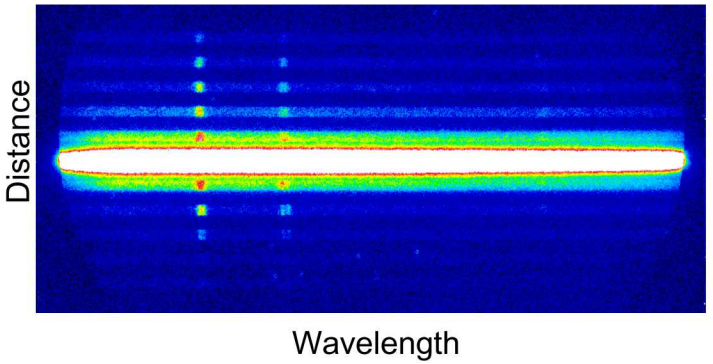

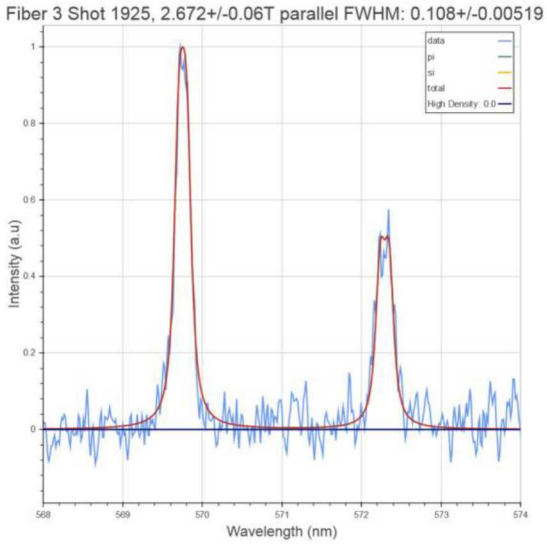

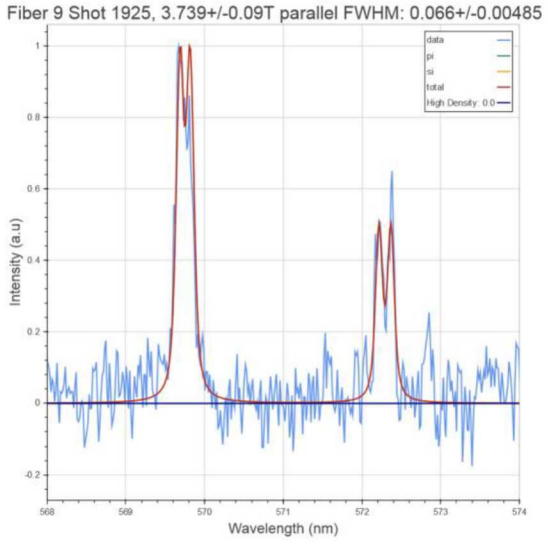

- Al thermal spray coated Tantalum target with small diameter cathode.
- Spectra taken at about (160 kA)
- Smaller cathode results in higher current densities.
- Splitting of Al III lines
- Asymmetric profile visible in the framing camera is quantified by the splitting of the spectra.
- Al dopant resulted in strong lines, and may be used to further localize fiber location

Shot 1960

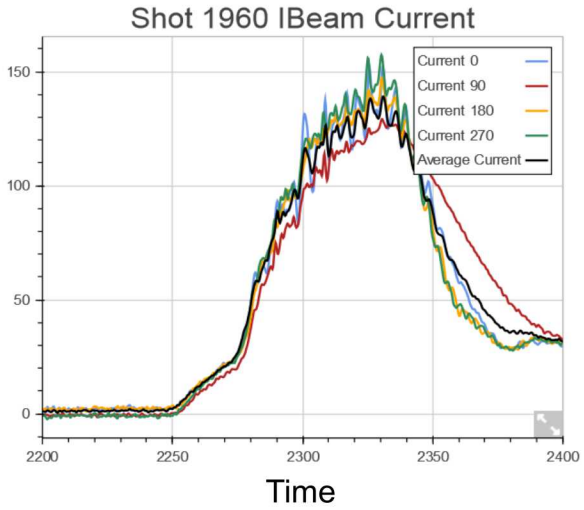

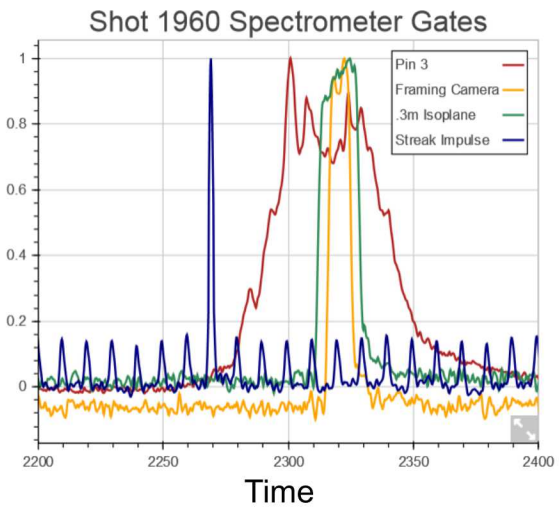

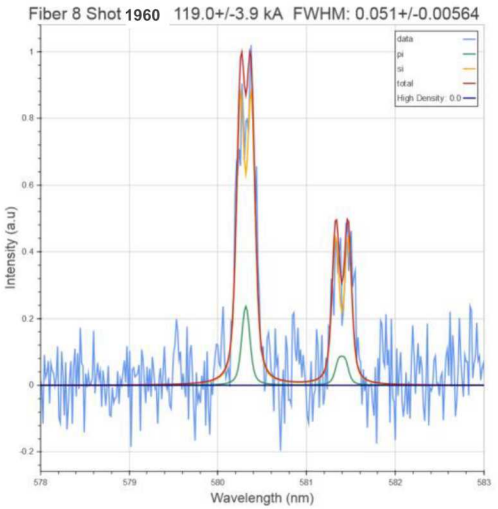

- Splitting has been measured on the standard SMP diode configuration with a Al foil
  - Al foil is used to prevent plasma expansion into the gap.

Enclosed Current

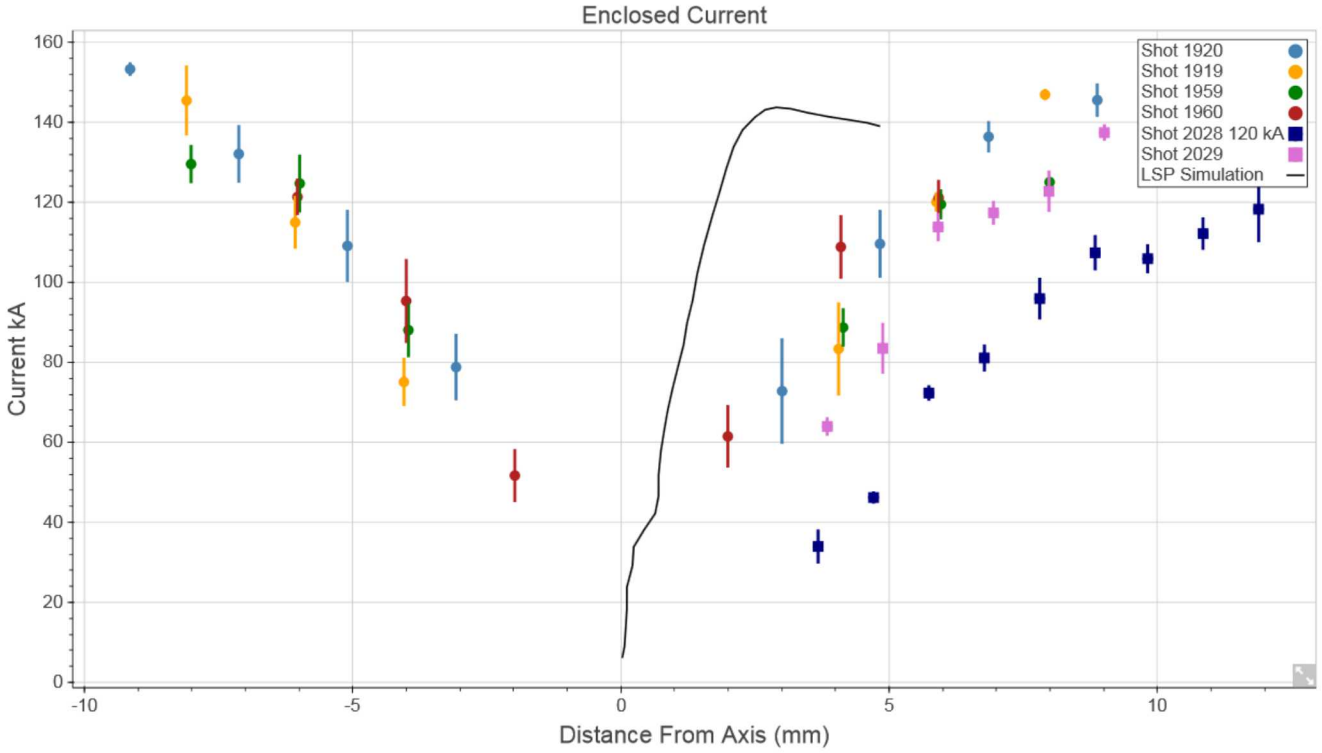

Simulation From N. Bennett

- Enclosed current increases roughly linearly with distance from the axis until about 8-10mm
- LSP simulation for a standard foil SMP diode (scaled to match shot current of 150 kA)
  - Just after the end of the radiation pulse.
  - Suggests more of the current is enclosed within a few mm region than the splitting measurements would suggest.

Current Density and B-Field

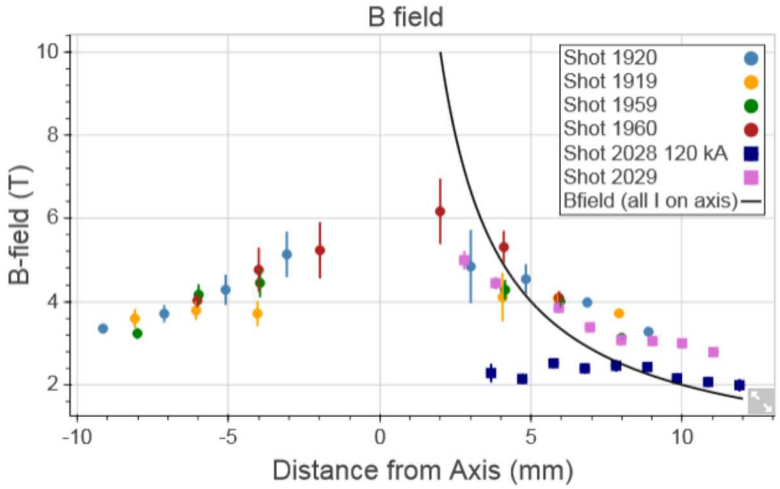

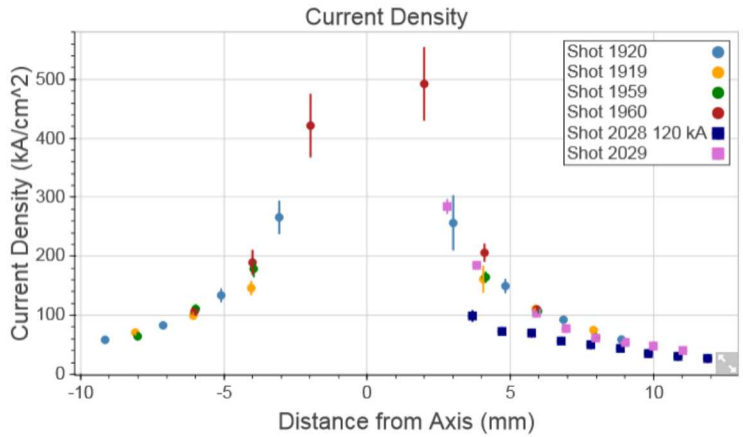

- Suggests B-field decreases linearly rather than 1/r.
- Shot 2028 showed a lot of spot motion and rapid expansion of the spot size.

Diamagnetic and Nernst Effects (possibly don't include)

Sandia National Laboratories

- Diamagnetic Drift:
  - $u_d = -\frac{\nabla p \times B}{qnB^2}$, depends on charge and so produces a current flow that cancels the external field.
  - Large temperature and density gradients exist close to the beam axis, and diamagnetic effects could partially shield the B-field
- Nernst Effect[9]:
  - Stronger than expected B fields were measured far from a laser focal spot[9]
  - The paper suggests this could be due to hot electrons which transport the fields generated by the laser away from the focal spot
  - Nernst velocity: $-2\left(n_e T_e \tau_{ei} \kappa^c \cdot \frac{\nabla T_e}{m_e}\right)\left(\frac{1}{5 n_e T_e}\right)$
  - $\dot{B} = -\nabla \times [(C + v_N) \times B]$, describes the evolution of the B-field with the Nernst velocity

9. L. Willingale, et al. PRL 105 (2010)

Dopants: Li

- Tantalum coated with LiF
- Strong Li lines were measured, however they were significantly broadened.
- Similar line widths across the fiber array suggests Li was measured at similar radii
- Li I is very susceptible to Stark shifts/broadening due to electric fields, and may be useful in the future to measure E fields
- Resulted in a standard radiation pulse length ~48 ns)

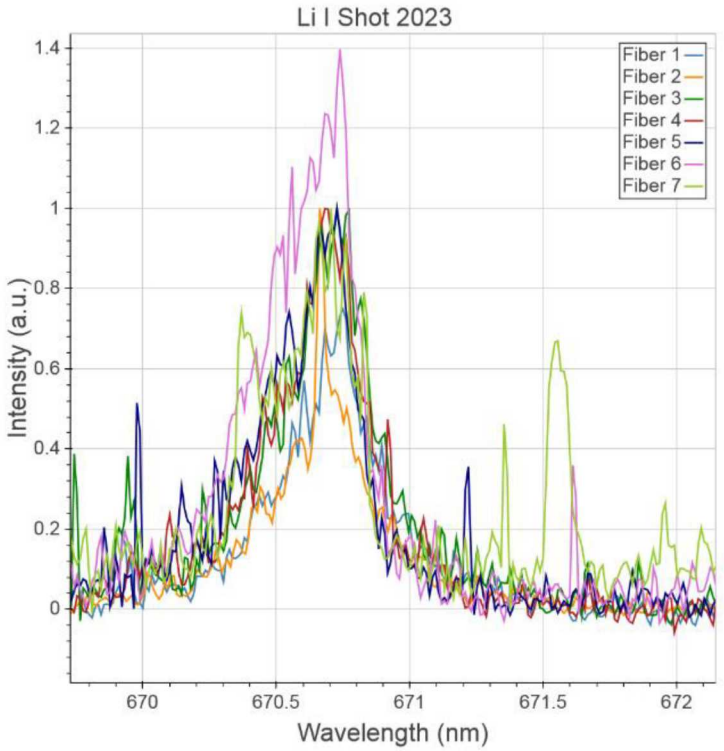

Dopants B and Si

- Not able to measure a high enough signal on either B III or Si IV
- Pulse lengths were shorter than on a normal foil shot, but comparable to a bare Ta shot ~35 ns

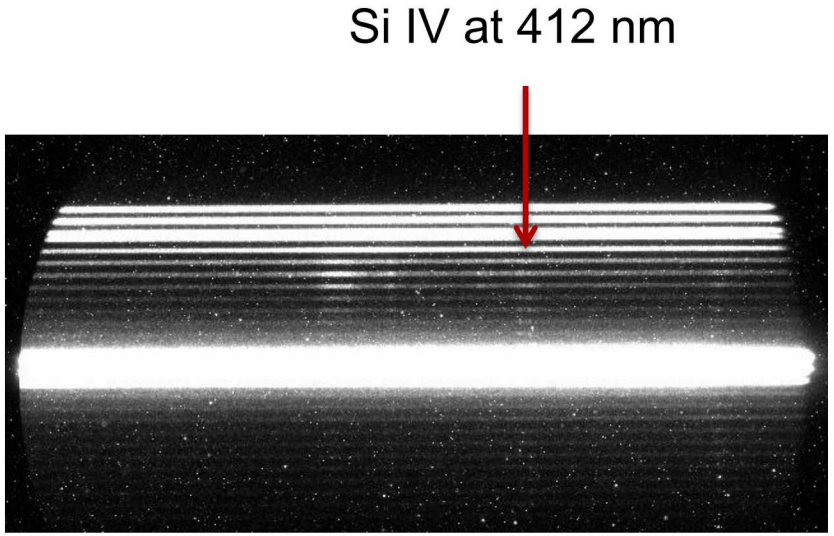

Dopants Al

- Strong signals were measured using a Al coated Ta target
- Zeeman splitting was measured on Al III at 569 and 572nm
- A Ta target with an Al strip along the center of the target showed strong lines and splitting as well, which will help further localize the measurement

Shot 2028, Al Coated Ta

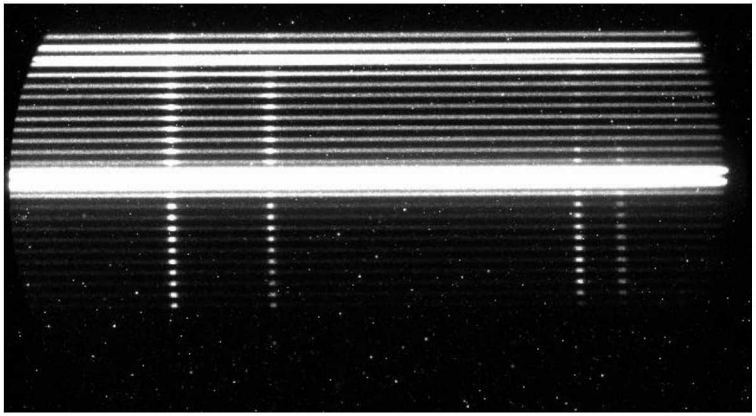

Shot 2046, 3mm Al Stripe

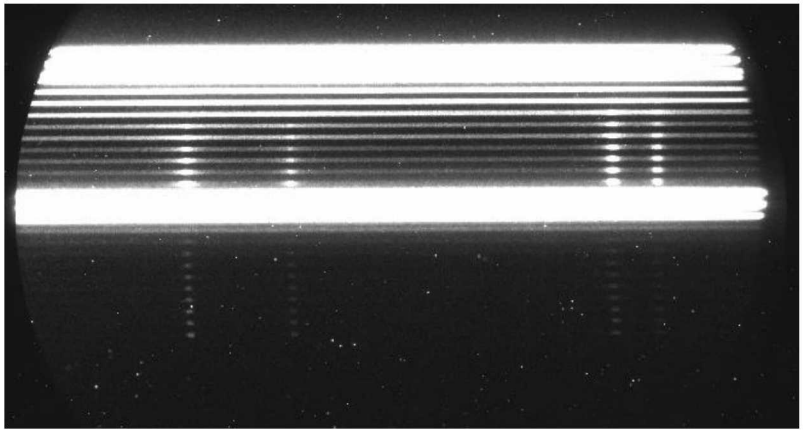

Z vs Radiation Pulse Length

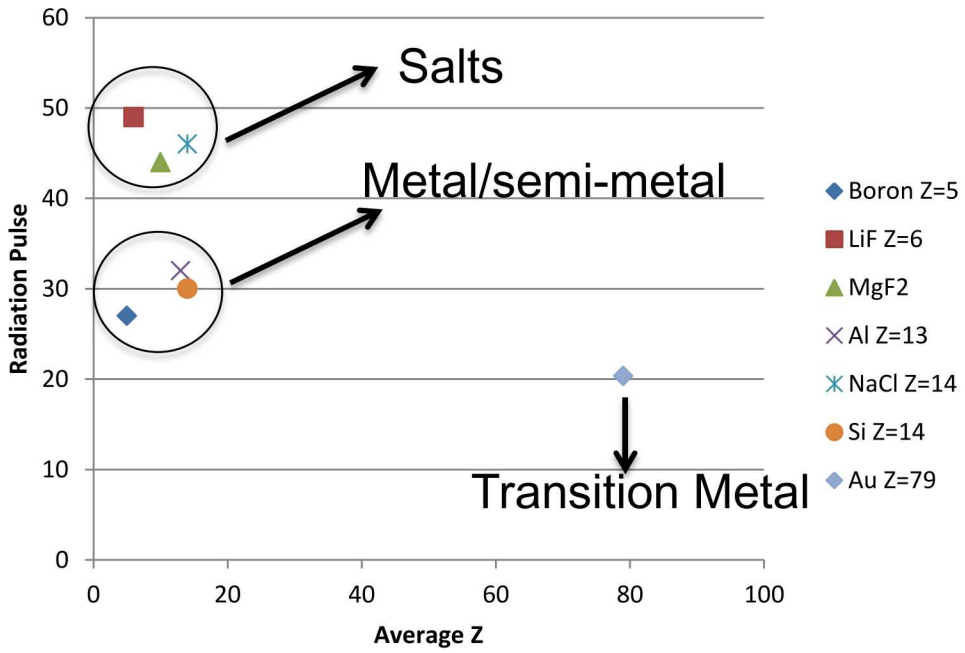

- Radiation pulse does not seem to depend on the atomic number of the coating
- Pulse lengths seem to be grouped by the type of material used in the coating. (add errors)

Future Work

Sandia National Laboratories

- Increase signal to noise to better resolve Zeeman splitting
- Use isolated dopants to more accurately spatially resolve the field distribution and increase SNR
- Further compare experimental data with LSP simulations
- Map magnetic fields and currents further into the gap
- Resolve the discrepancy between the expected current profiles and the data

Conclusions

Sandia National Laboratories

- Proof of principle B-field profile measurements have been made on RITS-6
  - Yields current distribution on the anode
- C IV and Al III line splitting has been measured.
- Densities has been estimated using PrismSPECT to fit Stark broadened lines
- These data suggests a large fraction of the total current may be outside a few mm radius

References

1. N. Bruner, D. Welch, K. Hahn, and B. Oliver, Phys. Rev. ST Accel. Beams 14, (2011)

2. N. Bennett, M. Crain, D. Droemer, et al. Phys. Rev. ST Accel. Beams 17, (2014)

3. N. Bennett, D.R. Welch, T.J. Webb, et al. Phys. Plasmas 22, (2015)

4. E. Stambulchik, K. Tsigutkin, and Y. Maron, PRL 98, (2007)

5. S. Tessarin, D. Mikitchuk, R. Doron, et al. Phys of Plasmas 18, (2011)

6. R.D. Cowan, *The theory of atomic structure and spectra* (1981)

7. H.R. Griem *Plasma Spectroscopy*, (1964)

8. K. Hahn, N. Bruner, S. Cordova, R. Gignac, M. Johnston, IEEE Trans. Plasma Sci, 38, (2010)